IN VITRO CYTOTOXICITY AND PHYSICOCHEMICAL EVALUATION OF FREEZE-DRIED HYDROGEL DELIVERY SYSTEMS OF HYDROCORTISONE

Kacper Odziomek[1]*, Sandra Komaniecka[1], Katarzyna Bialik-Wąs[2]*

[1] Cracow University of Technology,
Faculty of Chemical Engineering and Technology,
24 Warszawska St., 31-155 Cracow, Poland
[2] Cracow University of Technology,
Faculty of Chemical Engineering and Technology,
Department of Chemistry and Technology of Polymers,
24 Warszawska St., 31-155 Cracow, Poland
*e-mail: kacper.odziomek@student.pk.edu.pl,
katarzyna.bialik-was@pk.edu.pl

Abstract

Despite the diversity of available formulations for relieving topical symptoms of chronic skin diseases, inflammation, and hypergranulation tissue resulting from burn wounds, their efficacy is limited by side effects, application inconveniences, including the oiliness of the formulations, and the need for frequent application, which can affect patient compliance. Therefore, research has been carried out on freeze-dried hydrogel delivery systems of hydrocortisone, to evaluate their physicochemical (gel fraction, swelling ratio, pH and conductivity measurements), structural (FTIR), and morphological (SEM) properties, as well as their cytotoxicity (MTT tests). The gel fraction of freeze-dried hydrogel biomaterials (M-TH25 and M-TH50) reached 64% ± 0.3 and 63% ± 1.7, respectively, slightly higher than for the reference matrix (M) (61 ± 0.8). The swelling ratio (pH = 7.4) was in the range of 212–253% and 184–222%, respectively, comparable to the reference sample (208–277%). The incorporation of a thermosensitive polymeric nanocarriers (poly-N-isopropylacrylamide copolymers) containing hydrocortisone in the quantitative range 25–50 mg did not significantly change the overall morphology of the biomaterials. Both M and M-TH25 samples exhibit non-cytotoxicity towards mouse fibroblast cells BALB/3T3 (93% ± 10; 100% ± 8) and L929 (114% ± 8; 72% ± 10) cells with an observable variation in response for the M-TH25 sample, likely due to differences in cell behaviour and surface area. Importantly, M-TH50 sample shows cytotoxic effects (40% ± 5; 59% ± 4) mainly resulting from an excessively high concentration of the incorporated active substance. Further studies are planned (including on the release profile and kinetics of hydrocortisone and the assessment of the therapeutic effect), which may help to select an appropriate concentration of drug in the quantitative range 25-40 mg.

Keywords: *biomaterials, drug delivery system, hydrocortisone, freeze-drying, hydrogel*

[Engineering of Biomaterials 173 (2025) 03]

doi:10.34821/eng.biomat.173.2025.03

Submitted: 2025-04-05, Accepted: 2025-05-07, Published: 2025-05-12

Introduction

Hydrogels, as three-dimensional hydrophilic polymer networks, have the unique ability to absorb and hold significant amounts of biological fluids, such as wound secretions, while maintaining the desired properties [1]. Hydrogel biomaterials are still being widely studied because of their ability to provide a prolonged and controlled release of active substances [2], which should reduce the application frequency and cost of therapy, improve patient compliance, as well as increase the therapeutic effect [3]. One of the crucial natural polymers used in biomedicine is sodium alginate, a natural polysaccharide derived from marine brown algae. In the industry, it is mainly produced by *Macrocystis pyrifera*, *Ascophyllum nodosum* and *Laminaria spp*. as well as by some bacteria. Its discovery by Stanford in 1881 [4] opened the way for widespread use in a variety of industries, so it is now being explored in the form of tablets [5–7], microcapsules [8–10], and dressings [11–13] for prolonged release of active substances, as well as cell scaffolds [14–16], among others.

Freeze-dried hydrogels and lyogels can exhibit significant drug delivery advantages, including enhanced stability of formulations and incorporated medicines [17], improved thermal resistance [18] and prolonged release [19]. Moreover, freeze-drying is a widely used method for producing porous hydrogel scaffolds for tissue engineering [20,21]. Depending on the composition of the hydrogels and their desired applications, some challenges may arise, such as excessive brittleness or too slow swelling rates, sometimes requiring optimization. For example, lyoprotectants and cryoprotectants such as sugars, polyols, and amino acids are used [22,23]. The freeze-drying process for hydrogel drug delivery systems typically involves three critical stages: freezing, primary drying, and secondary drying. More complex techniques, such as the freeze–thaw cycling-annealing method, can further reorganize the hydrogels' cross-linking structure as well as simplify and accelerate hydrogels preparation [24]. Furthermore, spray freeze-drying is gaining traction for producing sustained-release particles of sizes and densities that show higher stability in the lungs, nasal mucosa, intestine, and skin, as compared to other drying technologies [25].

An interesting issue in the field of biomedical engineering is the use of hybrid biomaterials composed of both natural and synthetic polymers [26–29]. This combination ensures both biocompatibility and good mechanical strength of the obtained formulations [30–32], which can be designed to be lightweight, compact and tailored to suit specific body areas [33,34]. In comparison, traditional formulations, such as ointments and creams, have significant disadvantages that can hinder appropriate patient compliance [35]. These products can be greasy and leave undesirable residues on clothing and bedding, as well as prove uncomfortable for frequent topical applications, especially for active patients. All these features make hydrogels very desirable in biomedicine, including tissue engineering, drug delivery, and treatment of difficult-to-heal wounds and skin inflammations [36,37].

Particularly, the incorporation of hydrocortisone may be an interesting modification with high application potential. Hydrocortisone belongs to the group of glucocorticosteroids, having a characteristic four-ring arrangement. Specifically, it is based on a cyclopentanoperhydrophenanthrene core, which consists of three rings of six carbon atoms and one ring of five carbon atoms. It exhibits strong anti-inflammatory and immunosuppressive properties [38], making it a common choice for the treatment of skin diseases such as eczema and psoriasis [39–42], as well as other inflammatory conditions, including allergic rashes [43,44] and chronic wounds in patients with burns and hypergranulation tissue [45,46].

Hydrocortisone's mechanism of action involves the inhibition of pro-inflammatory factors as it diffuses through the stratum corneum and binds to cytoplasmic glucocorticoid receptors in keratinocytes, fibroblasts, and immune cells. The formed receptor-ligand complex then travels to the nucleus, where it binds genes containing regulatory sequences [47–49]. Activation of these sequences results in stimulation or inhibition of genes expression that are responsible for the synthesis of many important proteins [50]. Furthermore, studies have shown that corticosteroids, including hydrocortisone, can stabilize lysosomal membranes in activated immune cells, which can limit the release of lysosomal enzymes in areas affected by inflammation [51]. However, it is worth noting that the effectiveness of hydrocortisone may be limited by overly rapid absorption and metabolism, as well as potential systemic side effects [52]. The absorption of topical hydrocortisone depends on many factors, including the condition of the stratum corneum. Additionally, in the presence of inflammation, a damaged skin barrier can increase the penetration of corticosteroids [53]. Thus, it is crucial to select an appropriate method of its application.

To overcome these challenges, freeze-dried hybrid hydrogel biomaterials incorporated with a thermosensitive nanoparticle system containing hydrocortisone were obtained in this study. In the research part, characteristics of the hydrogel formulations (M-TH25 and M-TH50) were studied to evaluate their physicochemical, structural, and morphological properties. Their cytotoxicity on mouse fibroblast cells was also investigated under *in vitro* conditions.

Materials and Methods

N-isopropylacrylamide and N,N'-methylenebisacrylamide supplied by Sigma-Aldrich (Saint Louis, MO, USA), as well as gum arabic provided by POCH S.A. (Gliwice, Poland) were used for the synthesis of a thermosensitive polymeric nanocarrier. Sodium alginate (M_w = 12,000–40,000 g/mol), poly(ethylene glycol) diacrylate (PEGDA, M_n = 700 g/mol) and hydrocortisone, which were purchased from Sigma-Aldrich (Saint Louis, MO, USA), as well as poly(vinyl alcohol) (M_w = 72,000 g/mol), glycerin and ammonium persulfate acquired by POCH S.A. (Gliwice, Poland), were used to prepare hydrogel biomaterials. *Aloe Vera* lyophilizate was supplied by Zrób sobie krem (Prochowice, Poland), acetate buffer solution (pH = 4.5), phosphate buffer solution (pH = 7.4) and ammonium buffer solution (pH = 9.5) from Chempur (Piekary Śląskie, Poland), and ethyl alcohol (96%, v/v) from Fisher Scientific (Hampton, NH, USA). For cell culture and cell viability assays, Dulbecco's Modified Eagle's Medium (DMEM) - high glucose, penicillin-streptomycin, and L-glutamine solution (200 mM) were obtained from Sigma-Aldrich (Saint Louis, MO, USA). NewBorn Calf Serum and Advanced MEM were supplied by Gibco™ (Waltham, MA, USA), and fetal bovine serum was purchased from Biowest (Nuallé, France).

Synthesis of a thermosensitive polymeric nanocarrier

The thermosensitive polymeric nanocarrier was obtained by emulsion polymerization of N-isopropylacrylamide and N,N-methylenebisacrylamide. Firstly, a 0.5% gum arabic solution was prepared in a three-neck round-bottom flask, which was then placed in a glycerin bath. Then, N-isopropylacrylamide and N,N-methylenebisacrylamide were added to the flask. The flask contents were heated to 70°C in an inert gas atmosphere with continuous stirring. Finally, ammonium persulfate was introduced, and the reaction mixture was heated at 80°C for 4 h. The obtained nanocarrier was purified by dialysis using a cellulose membrane (MWCO = 14,000 Da) [54,55,18,56,26].

Encapsulation of hydrocortisone in a thermosensitive polymeric nanocarrier

The encapsulation procedure was initiated by adding the respective amounts, i.e., 25 mg (TH25) and 50 mg (TH50) of hydrocortisone dissolved in ethyl alcohol, to the purified thermosensitive polymeric nanocarrier. The solution was placed in a round-bottom flask and stirred intensively at a constant speed of 1200 rpm at room temperature for 3 h. The obtained system was freeze-dried for 24 h [18,56,26].

Preparation of hydrogel biomaterials incorporated with a thermosensitive nanocarrier-hydrocortisone system

In order to prepare hydrogel biomaterials, a 5% (*w/v*) poly(vinyl alcohol) solution, a 2% (*w/v*) sodium alginate solution, a 2% (*w/v*) *Aloe vera* solution, and a 1% (*w/v*) ammonium persulfate solution were prepared. Then the freeze-dried thermosensitive nanocarrier-hydrocortisone system was dispersed in a 2% (*w/v*) aqueous sodium alginate solution [57]. All solutions in appropriate volumes were mixed with constant amounts of PEGDA (7.5%, *v/v*) and glycerin (1.7%, *v/v*). Details on the reaction mixtures' composition were included in previous studies [18,26,56,58–62]. The mixtures were heated to 70°C and a 4.4% (*v/v*) ammonium persulfate solution was added. The samples were poured then into Petri dishes and placed on a heating plate. The cross-linking reaction was carried out at 80°C for 1.5 h. Thus, a series of samples were prepared with different hydrocortisone concentrations: 0 mg (M), 25 mg (M-TH25) and 50 mg (M-TH50), which were then left for 48 h under ambient conditions. For complete removal of unbound water, the samples were frozen at −18°C for 24 h and then subjected to freeze-drying in a ChristAlpha 1−2 LD Plus freeze-dryer (Martin Christ, Osterode am Harz, Germany) at −53°C under 0.2 mBa.

Determination of the gel fraction

The dried hydrogel biomaterials (M-TH25 and M-TH50) were cut into smaller 10 × 10 mm pieces and then weighed (W_0). The samples were immersed in distilled water for 48 h to remove any easily leachable or soluble parts. Finally, the hydrogels were dried at 40°C for 24 h and weighed again (W_E). The gel fraction (%GF) was determined using the following equation (1):

$$\%GF = (W_E/W_0) \cdot 100\% \quad (1)$$

Determination of the swelling ratio

The dried hydrogel biomaterials (M-TH25 and M-TH50) were cut into smaller 10 × 10 mm pieces and then weighed (W_D). The samples were immersed in acetate buffer solution (pH = 4.5), phosphate buffer solution (pH = 7.4) and ammonium buffer solution (pH = 9.5) at 37°C. The swollen hydrogels were taken out and weighed (W_S) after 1, 2 and 24 h. The swelling ratio (%SR) was determined using the following equation (2):

$$\%SR = (W_S - W_D)/W_D \cdot 100\% \quad (2)$$

pH and conductivity measurements

Samples of hydrogel biomaterials (M, M-TH25 and M-TH50) weighing 250 mg were placed in 50 mL of acetate buffer solution (pH = 4.5), phosphate buffer solution (pH = 7.4) and ammonium buffer solution (pH = 9.5), and then incubated at 37°C. The pH and conductivity of the incubation fluids were measured over the 23-day incubation period using a conductometer and a pH meter equipped with a glass electrode.

Attenuated total reflectance-Fourier transform infrared spectroscopy (ATR-FTIR)

To identify the chemical structure of the hydrogel biomaterials (M-TH25 and M-TH50), a Thermo Scientific Nicolet iS5 FT-IR spectrophotometer (Thermo Fisher Scientific, Waltham, MA, USA) equipped with an iD7 ATR accessory in the range of 4000–400 cm^{-1} was used.

Scanning electron microscopy (SEM)

The morphology of the hydrogel biomaterials (M-TH25 and M-TH50) was analyzed using an Apreo 2 S LoVac scanning electron microscope (Thermo Fisher Scientific, Waltham, MA, USA) equipped with an EDS UltraDry and Octane Elect detectors (EDAX Ametek GmbH, Weiterstadt, Germany). The samples were sputter-coated with a 2.5 nm layer of gold in an argon atmosphere. The analysis was carried out under high vacuum conditions.

Cell culture

Mouse fibroblast cells BALB/3T3 were purchased from the American Type Culture Collection (ATCC, Manassas, VA, USA), while L929 cells were purchased from the European Collection of Authenticated Cell Cultures (ECACC, Porton Down, UK). To obtain an appropriate number of cells for analysis, BALB/3T3 and L929 fibroblasts were cultured in a complete medium composed of, respectively: DMEM, 10% NBCS, 1% Pen/Strep, 4 mM L-glutamine, and EMEM, 10% FBS, 1% Pen/Strep, 2 mM L-glutamine, in T-75 culture flasks. Culture medium was replaced every 3 days with fresh medium, while passages were conducted at culture confluences reaching 70–80%. Cell counts and viability after passages were monitored using an ADAM™MC cell counter (NanoEntek, Guro-gu, Seoul, Korea). After obtaining an appropriate count of BALB/3T3 cells at the thirteenth passage and L929 cells at the sixth and seventh passages, fibroblast cultures were established in a 96-well plate (104 cells per well), with the outer wells of the plate serving as a blank.

Cell viability assays

In order to study the cytotoxicity of biomaterials (M, M-TH25 and M-TH50), in vitro tests were carried out on the mouse fibroblast cell lines (BALB/3T3 and L929). First, biomaterial extracts (M, M-TH25 and M-TH50) were prepared in serum-reduced test medium composed of: DMEM, 5% NBCS, 1% Pen/Strep, 4 mM L-glutamine (BALB/3T3) and EMEM, 5% FBS, 1% Pen/Strep, 2 mM L-glutamine (L929). Biomaterials extraction was carried out for 24 h. After 24 h of cell culture establishment, 100 µL of biomaterials extracts were added to each well of the plates, each extract in 6 replicates. The plates were incubated at 37°C in a humidified atmosphere containing 5% CO_2 for 24 h. After this time, the extracts were removed from above the cells and cell viability was determined using the MTT assay. For this purpose, MTT stock with a concentration of 5 mg/mL was dissolved in a complete medium to make its final concentration 0.5 mg/mL, and then 100 µL was added to each well containing cells and incubated for 3 h at 37°C in a humidified atmosphere containing 5% CO_2. After incubation, the MTT solution was removed from above the culture and 100 µL of isopropanol was added to each well (including the blank). Then, the contents were shaken for 15 min to dissolve the formazan crystals formed and obtain a homogeneous solution. Finally, the plates were placed in a Spark 10 M microplate reader (Tecan, Männedorf, Switzerland), where absorbance was measured at 570 nm for each well. A negative control (BALB/3T3 and L929 cells incubated with culture medium) and a positive control (L929 cells incubated with 1% SDS) were also analyzed.

Statistical analysis

The data from the determination of the gel fraction and swelling ratio were presented as mean values of three different experiments ± SD, while data related to cell viability assays are presented as mean values of six different experiments ± SD. Differences between the calculated means of each individual group were determined by one-way ANOVA tests using the statistical software Statistica Version 12 from StatSoft Company (Cracow, Poland). The value of $p < 0.05$ was considered statistically significant.

Results and Discussions

Physicochemical analysis

The gel fraction of hydrogel biomaterials (M-TH25 and M-TH50) is presented in FIG. 1a, while swelling ratio of hydrogel biomaterials (M-TH25 and M-TH50) is presented in FIG. 1b.

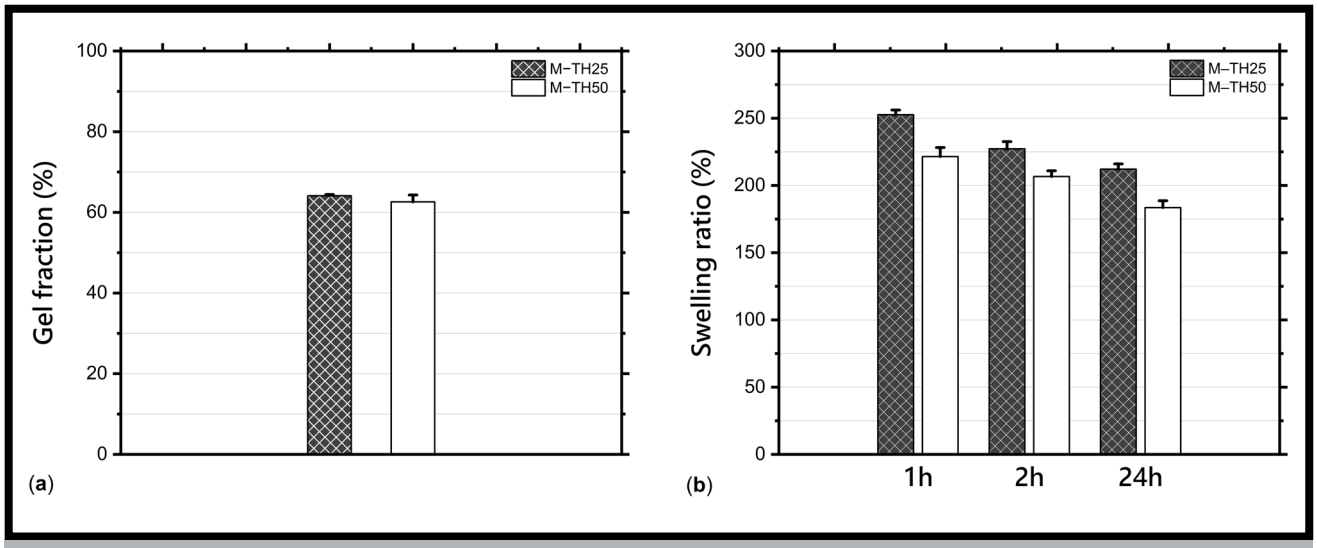

FIG. 1. Gel fraction (a) and swelling ratio (b) of the analyzed hydrogel biomaterials (M-TH25 and M-TH50). The results are presented as mean values (*n* = 3), while the bars represent ± SD.

The gel fraction of hydrogel biomaterials (M-TH25 and M-TH50) reached 64% ± 0.3 and 63% ± 1.7, respectively, while the gel fraction of the reference sample (M) was 61 ± 0.8 which was determined in the previous research paper [18]. This implies that the introduction of a thermosensitive polymeric nanocarrier-hydrocortisone system may slightly impact the value of the gel fraction of the analyzed formulations. This phenomenon is well documented in the literature, according to which even small variations in the concentration of the incorporated active substance or the presence of other additional components can result in some differences in the degree of cross-linking [63]. Furthermore, an additional stabilizing procedure of hydrogel formulations, such as sublimation drying, can result in more extensive phase separation and crystallization of poly(vinyl alcohol), as well as enhancement of physical interactions between polymer chains [18]. The highest value was observed for the hydrogel biomaterial containing 25 mg of hydrocortisone (M-TH25), while the lowest value was recorded for the reference sample without the drug (M). However, it is important to emphasize that the minimal differences between the gel fraction of the samples (M-TH25 and M-TH50) are within the range of measurement error. Significantly, an increase in the number of cross-linking bonds of a hydrogel allows to improve its mechanical properties and stability, but too high degree of cross-linking can simultaneously limit the swelling and release of active substances [64]. Therefore, an analysis of the swelling ratio of biomaterials (M-TH25 and M-TH50) was carried out to choose the optimal amount of hydrocortisone.

The swelling ratio of hydrogel biomaterials (M, M-TH25 and M-TH50) in a buffer solution of pH = 7.4 was in the range of 208–277% (mean ± 4.6–17.9%) [18], 212–253% (mean ± 3.5–5.3%) and 184–222% (mean ± 4.3–6.7%), respectively. According to the results achieved, it was found that the swelling ratio of the samples decreases with incubation time. It is supported by literature data, according to which most hydrogels show an initial increase in swelling followed by a slight decrease. The observed phenomenon can be due to changes in the polymer network, which can result from leaching of the active substances present in *Aloe vera* and hydrocortisone from the samples, as well as alterations in the osmotic balance. The highest swelling ratio was observed for the reference sample (M) and the lowest for the biomaterial incorporated with a system composed of a thermosensitive polymeric nanocarrier and 50 mg of hydrocortisone (M-TH50). The swelling properties of hydrogel formulations can vary depending on their chemical composition and the degree of cross-linking which has a significant effect on the number of hydrophilic groups, as well as on the release profile of the present active substances [65–67].

pH and conductivity measurements

The changes in conductivity and pH of the incubation fluids in which the hydrogel biomaterials (M, M-TH25 and M-TH50) were put are presented in FIGs 2 and 3.

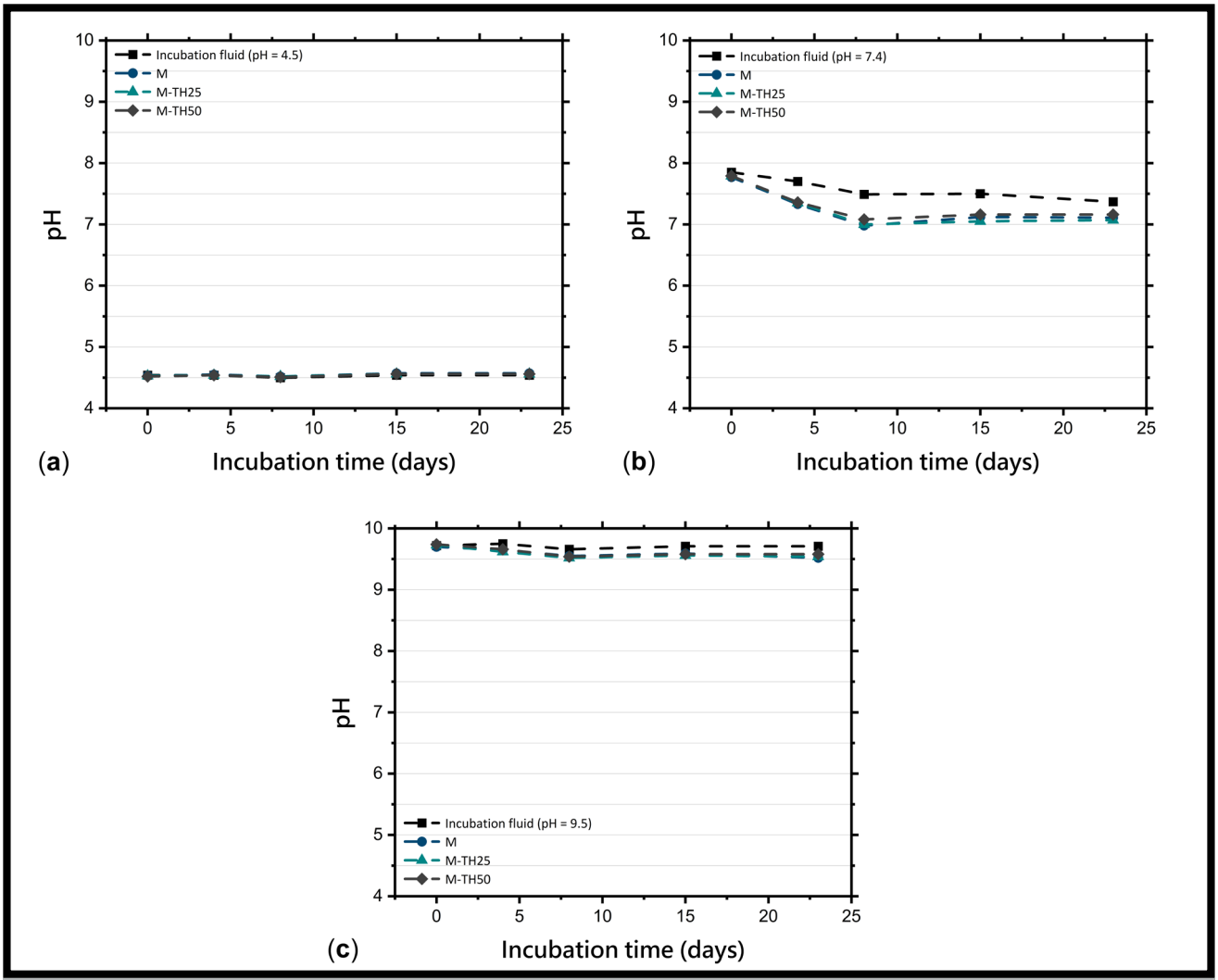

FIG. 2. Changes in the pH of incubation fluids with a nominal value: (a) 4.5; (b) 7.4; (c) 9.5.

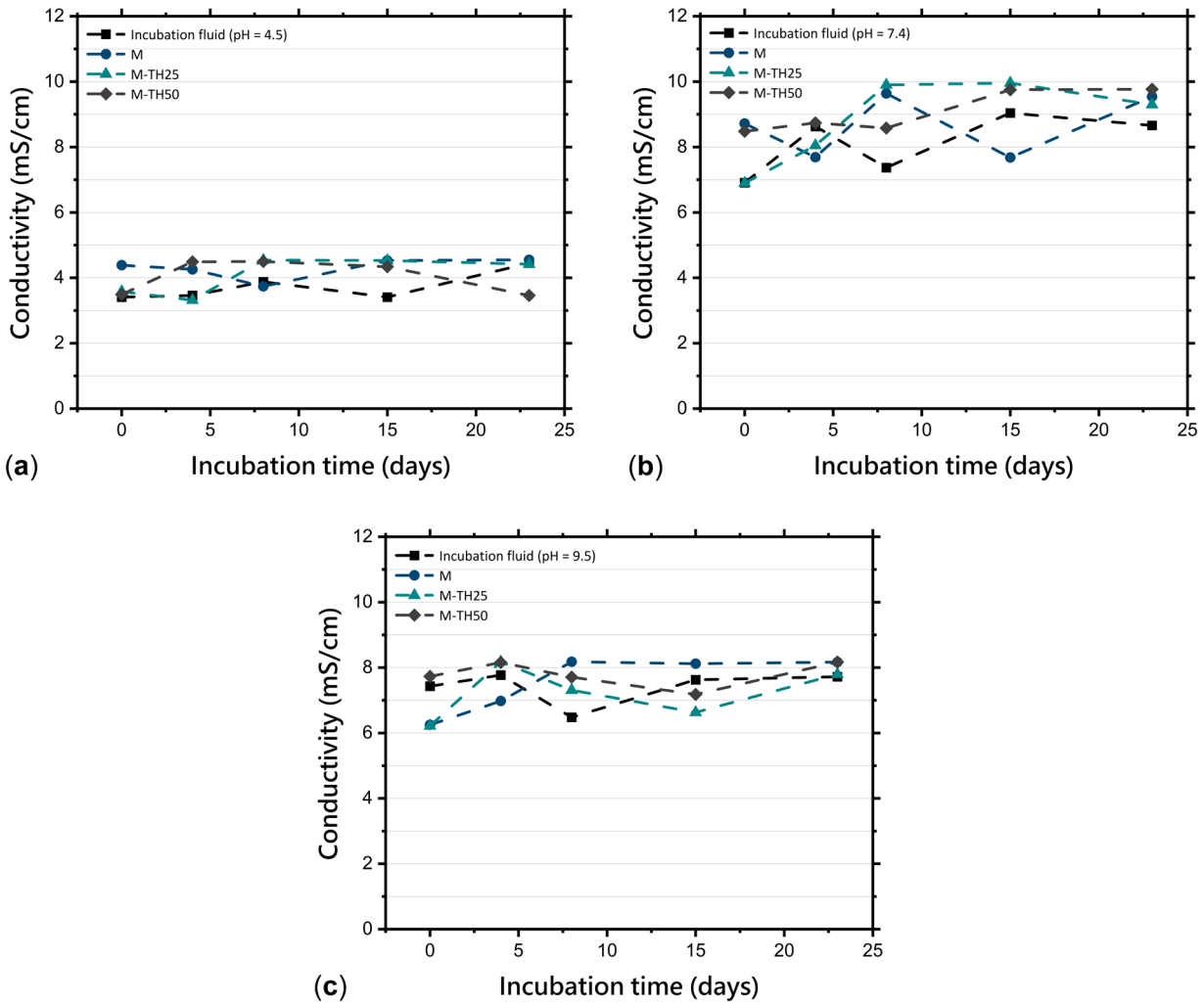

FIG. 3. Changes in the conductivity of incubation fluids with pH: (a) 4.5; (b) 7.4; (c) 9.5.

The pH of the incubation fluids with an initial value of 4.5, was observed to remain constant. As proven in a previous study [18], low environmental pH can limit swelling of the samples and, consequently, ion exchange. In a neutral environment (pH = 7.4), a slight tendency to decrease pH in the presence of hydrogel biomaterials is visible, which may be related to ion release and suggest a minor degradation of the matrices. No significant changes were observed at pH = 9.5. Minimal variations in the range of 0.1–0.2 confirm that no significant change in the ionic composition of the solution occurs in an alkaline environment.

The conductivity values of the fluids at pH = 4.5 were observed to maintain a similar level throughout the entire incubation period. The slight increase or decrease at specific measurement points may be related to the very slow release of ions from the inside of biomaterial. The conductivity value of the reference fluid at pH = 7.4 was initially 6.9 mS/cm and increased to 8.7 mS/cm with time. After the introduction of hydrogel biomaterials (M, M-TH25, and M-TH50), a small growth in conductivity was also observed, especially for fluids in which samples containing the nanocarrier-drug system (M-TH25 and M-TH50) were incubated, indicating its release. Importantly, on the 23rd day of analysis, a stabilization tendency was noticed, which confirms that an equilibrium state has been reached.

Analysis of the results confirms the stability of the tested biomaterials over a wide pH range. Minor changes may result from partial ion exchange, release of hydrocortisone, and in the case of a pH = 7.4 environment, slight degradation of hydrogel biomaterials.

FT-IR analysis

The FT-IR spectra of hydrogel biomaterials (M-TH25 and M-TH50) as well as the identification of their bands are presented in FIG. 4 and TABLE 1, respectively.

Analysis of FT-IR spectra confirmed the presence of the functional groups characteristic of the hydrogel biomaterials studied. An intense band was observed at a wavenumber of ~3300 cm^{-1}, which corresponds to the stretching vibrations of O-H hydroxyl groups present in the structure of sodium alginate, poly(vinyl alcohol) and *Aloe vera*. In the wavenumber range of 2940–2912 cm^{-1}, bands of lower intensity were noted, originating from asymmetric stretching vibrations of the C-H groups. Furthermore, a clear band in the wavenumber range of 1730–1715 cm^{-1}, derived from C=O stretching vibrations, confirms the presence of carboxyl groups bonded to alginate acids rings, which form ester bonds during the cross-linking reaction of biomaterials using poly(ethylene glycol) diacrylate. The peaks originating from the stretching vibrations of the C-O-C groups, related to the use of PEGDA as a cross-linking agent, were also observed at 1090 cm^{-1}.

Moreover, a band reaching a maximum at 1035 cm^{-1} was noticed, resulting from both the presence of C-O-C, as well as C-O and C-OH bonds, contained in the structure of sodium alginate and *Aloe vera*. The bands at wavenumbers of 1611 cm^{-1} and 1423 cm^{-1} were assigned to asymmetric and symmetric stretching vibrations of the COO- carboxylate anion. On the other hand, the band in the range of 1647–1608 cm^{-1} comes from C=C stretching vibrations of hydrocortisone. Additionally, the band at a wavenumber of 1375 cm^{-1} was found to be related to CH_2 vibrations from the aliphatic chain of poly(vinyl alcohol), and the band within 1251–1261 cm^{-1} was attributed to C-O-C vibrations from glycosidic bonds connecting the sugar residues of polysaccharides.

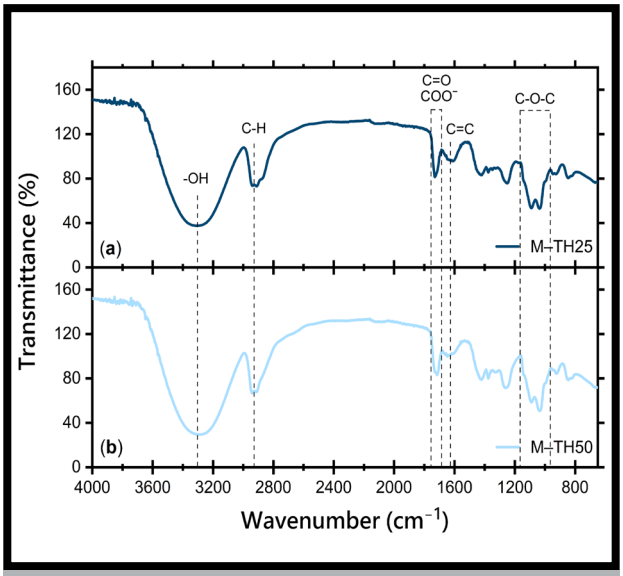

FIG. 4. FT-IR spectra of hydrogel biomaterials: (a) M-TH25; (b) M-TH50.

Considering the FT-IR data for the reference sample (M) achieved in the previous paper [18], it can be concluded that the incorporation of the nanocarrier-hydrocortisone system into hydrogel biomaterials does not interfere with their chemical structure. Only slight shifts in the 3288–3311 cm^{-1} and 1647–1608 cm^{-1} region, typical of weak hydrogen bonds, were observed. The potential interactions between SA, PVA, *Aloe vera*, the nanocarrier-hydrocortisone system, and PEGDA are presented in FIG. 5.

TABLE 1. Identification of FT-IR spectra bands of hydrogel biomaterials (M-TH25 and M-TH50).

Identification	Wavenumber (cm^{-1})	
	M-TH25	M-TH50
O-H stretching vibration	3311	3288
C-H asymmetric stretching vibration	2912	2940
C=O stretching vibration	1730	1715
C=C asymmetric stretching vibration	1608	1647
C=C symmetric stretching vibration	1423	1423
CH_2 wagging vibration	1375	1375
C-O-C vibration from glycosidic bonds	1251	1261
C-O-C stretching vibration	1090	1090
C-C stretching vibration C-O-C vibration from glycosidic bonds	1036	1035

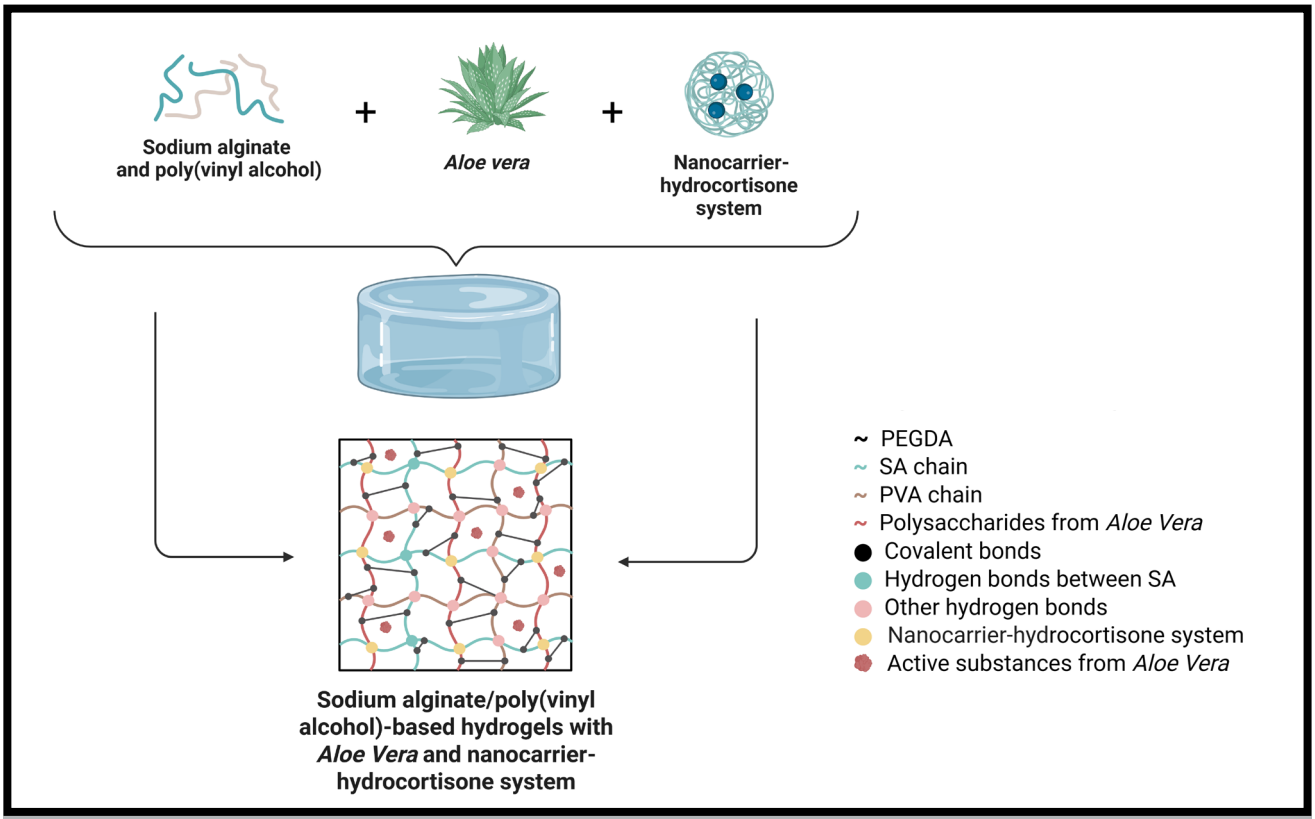

FIG. 5. The potential interactions between SA, PVA, *Aloe vera*, the nanocarrier-hydrocortisone system and PEGDA.

SEM analysis

The cross-sectional SEM images of hydrogel biomaterials (M-TH25 and M-TH50) are presented in FIG. 6.

According to cross-sectional SEM images of hydrogel biomaterials, some morphological differences were observed. As proven in the previous study, the reference sample without active substance (M) was characterized by a relatively dense structure with a considerable number of small pores, which can result in the lowest gel fraction value among all tested hydrogels, at 61 ± 0.8 [18]. No significant alterations were observed for the M-TH25 sample. However, the introduction of a thermosensitive polymeric nanocarrier containing a higher concentration of hydrocortisone into the biomaterial results in the appearance of more pronounced channels in the cross-section. The hydrogel biomaterial (M-TH50) exhibits a more expanded and differentiated structure with distinct cavities, which is most visible at a magnification of 5,000× (FIG. 6D). The drug molecules can be seen in FIG. 6H, which partially fill the empty pores in the hydrogel structure, possibly reducing the swelling ratio of the analyzed sample (FIG. 1b). Nevertheless, the structural integrity in both cases is well preserved, suggesting that the incorporation of a thermosensitive polymeric nanocarrier containing hydrocortisone in the 25–50 mg quantitative range does not significantly change the overall morphology of biomaterials.

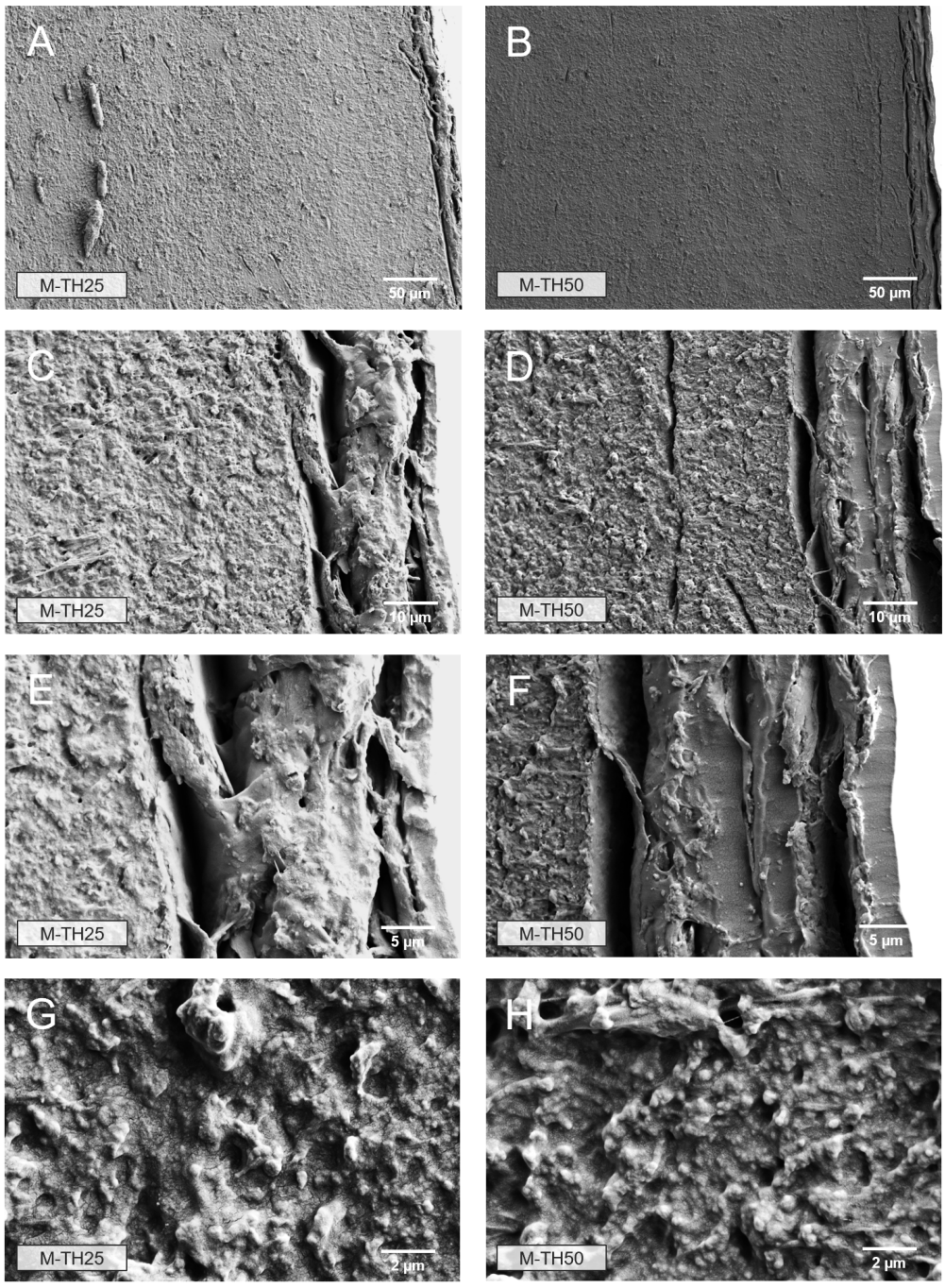

FIG. 6. The cross-sectional SEM images of the hydrogel biomaterial (M-TH25) at magnifications: (a) 1,000×; (c) 5,000×; (e) 10,000×; (g) 20,000×, as well as of the hydrogel biomaterial (M-TH50) at magnifications: (b) 1,000×; (d) 5,000×; (f) 10,000×; (h) 20,000×.

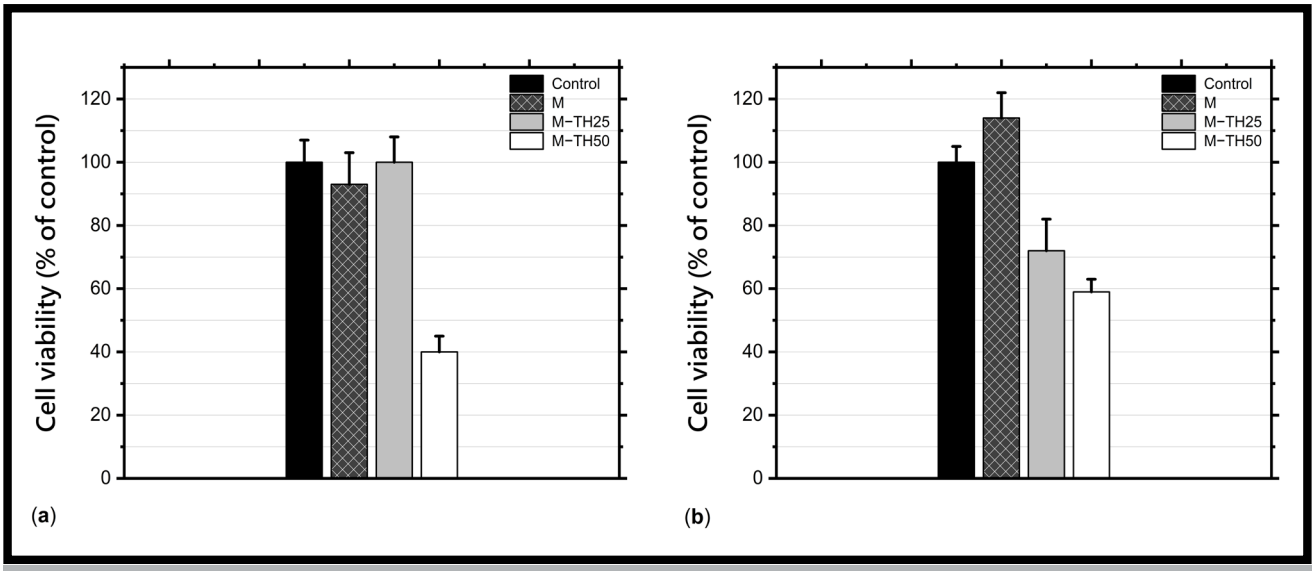

FIG. 7. The viability of: (a) BALB/3T3 and (b) L929 cells in the presence of hydrogel biomaterials (M, M-TH25 and M-TH50) after 24 h of incubation. The results are presented as mean values (*n* = 6), while the bars represent ± SD.

Cell viability analysis

The viability of BALB/3T3 and L929 cells in the presence of hydrogel biomaterials (M, M-TH25, and M-TH50) after 24 h of incubation is presented in FIG. 7.

The cytotoxicity evaluation of hydrogel biomaterials (M, M-TH25, and M-TH50) on BALB/3T3 and L929 cell lines was performed following ISO 10993-5 guidelines [68] to assess their biocompatibility for potential biomedical applications. According to ISO 10993-5, a material is considered to be safe if cells cultured with the extract (a medium suitable for specific cells, pre-conditioned for a period of 24 h in direct contact with the tested material), exhibit metabolic activity >70% with respect to a standard control group. BALB/3T3 cells after 24 h of incubation in the presence of a reference sample (M) exhibited a viability of 93% ± 10, which indicates a lack of cytotoxic effect. Interestingly, cell viability was maintained at 100% ± 8 for the M-TH25 biomaterial, confirming its non-cytotoxicity. However, a strong cytotoxic effect was noted for the M-TH50 sample, which decreased cell viability to a value of 40% ± 5 by direct contact. In comparison, L929 cells showed a slightly different response to contact with the formulations. While the cells after 24 h of incubation in the presence of a reference sample (M) demonstrated a viability of 114% ± 8, potentially indicating a proliferative effect, exposure to M-TH25 sample resulted in a major decrease in cell viability. Viability in the presence of M-TH25 biomaterial reached 72% ± 10, while in the presence of M-TH50 it was 59% ± 4, which confirms its cytotoxicity.

In conclusion, M and M-TH25 biomaterials exhibit non-cytotoxicity towards BALB/3T3 and L929 cells in compliance with ISO 10993-5 standards. However, the cytotoxicity assay of the M-TH25 sample revealed a difference in response between the BALB/3T3 and L929 cell lines, which can be attributed to differences in cell behaviour and surface area. Importantly, M-TH50 sample shows cytotoxic effects, mainly resulting from an excessively high concentration of the incorporated active substance. Therefore, future work will include attempts to select an appropriate drug concentration in the 25–40 mg quantitative range with additional consideration of the release profile and kinetics, as well as the therapeutic effect.

Conclusions

The gel fraction of biomaterials (M-TH25 and M-TH50) reached similar values, but slightly higher than the reference sample (M), suggesting a dependence of this value on the presence of additional components, such as active substances. The swelling ratio of the samples decreased with incubation time, which can be due to some changes in the polymer network, possibly resulting from leaching of the active substances present in *Aloe vera* and hydrocortisone from the samples, as well as alterations in the osmotic balance. The pH and conductivity measurements confirmed the stability of the formulations over a wide pH range. The chemical structure of the obtained biomaterials was confirmed by FT-IR analysis. Small shifts in the 3288–3311 cm^{-1} and 1647–1608 cm^{-1} regions may be related to the appearance of additional weak hydrogen bonds. Interestingly, the M-TH50 sample had a more expanded and differentiated structure with more pronounced cavities. The slight morphological changes can be caused by the difference in the amount of drug introduced and do not disturb their overall morphology. The in vitro cytotoxicity assessment of the materials clearly indicated that M and M-TH25 are not toxic to mouse fibroblast cells. However, the cytotoxicity assay of the M-TH25 sample revealed a difference in response between the BALB/3T3 and L929 cell lines, probably due to differences in cell behaviour and surface area. The M-TH50 sample shows cytotoxic activity, resulting from an excessive concentration of introduced hydrocortisone. Based on the results, it can be concluded that freeze-dried hydrogel delivery systems of hydrocortisone with high application potential in biomedicine have been obtained. Further studies are planned, which may help to select an appropriate concentration of the drug in the quantitative range of 25–40 mg, including the release profile and kinetics, as well as the evaluation of the therapeutic effect.

Acknowledgements

This work was co-financed by the Ministry of Science and Higher Education within the project no. W220 "Hydrogel drug delivery systems for terrestrial and space medicine", which received funding from the non-competitive project "Support for students to improve their competencies and skills" no. FERS.01.05-IP.08-004/23 (Measure 01.05 Skills in Higher Education, European Funds for Social Development 2021–2027 Programme). Moreover, we would like to thank Przemysław Woliński, M. Eng. for the professional SEM imaging carried out at the Research Laboratory of the Cracow University of Technology's Faculty of Chemical Engineering and Technology.

References

[1] Brannon-Peppas L.: Preparation and Characterization of Crosslinked Hydrophilic Networks. Studies in Polymer Science 8 (1990) 45-66.
[2] Peppas N.A., Hilt J.Z., Khademhosseini A., Langer R.: Hydrogels in Biology and Medicine: From Molecular Principles to Bionanotechnology. Advanced Materials 18 (2006) 1345-1360, doi:10.1002/adma.200501612.
[3] Jayakumar A., Jose V.K., Lee J.-M.: Hydrogels for Medical and Environmental Applications. Small Methods 4 (2020) 1900735, doi:10.1002/smtd.201900735.
[4] Smith W.: Report on the Exhibits Relating to the Chemical Industries, in the International Inventions Exhibition, wyd. Emmott, London 1885.
[5] Sanchez-Ballester N.M., Bataille B., Soulairol I.: Sodium Alginate and Alginic Acid as Pharmaceutical Excipients for Tablet Formulation: Structure-Function Relationship. Carbohydrate Polymers 270 (2021) 118399, doi:10.1016/j.carbpol.2021.118399.
[6] Jin L., Qi H., Gu X., Zhang X., Zhang Y., Zhang X., Mao S.: Effect of Sodium Alginate Type on Drug Release from Chitosan-Sodium Alginate-Based In Situ Film-Forming Tablets. AAPS PharmSciTech 21 (2020) 55, doi:10.1208/s12249-019-1549-y.
[7] Huq T., Vu K.D., Riedl B., Bouchard J., Han J., Lacroix M.: Development of Probiotic Tablet Using Alginate, Pectin, and Cellulose Nanocrystals as Excipients. Cellulose 23 (2016) 1967-1978, doi:10.1007/s10570-016-0905-2.
[8] Noppakundilograt S., Piboon P., Graisuwan W., Nuisin R., Kiatkamjornwong S.: Encapsulated Eucalyptus Oil in Ionically Cross-Linked Alginate Microcapsules and Its Controlled Release. Carbohydrate Polymers 131 (2015) 23-33, doi:10.1016/j.carbpol.2015.05.054.
[9] Tian Y., Liu Y., Zhang L., Hua Q., Liu L., Wang B., Tang J.: Preparation and Characterization of Gelatin-Sodium Alginate/Paraffin Phase Change Microcapsules. Colloids and Surfaces A: Physicochemical and Engineering Aspects 586 (2020) 124216, doi:10.1016/j.colsurfa.2019.124216.
[10] Saenz del Burgo L., Ciriza J., Espona-Noguera A., Illa X., Cabruja E., Orive G. et al.: 3D Printed Porous Polyamide Macrocapsule Combined with Alginate Microcapsules for Safer Cell-Based Therapies. Scientific Reports 8 (2018) 8512, doi:10.1038/s41598-018-26869-5.
[11] Kim J.O., Park J.K., Kim J.H., Jin S.G., Yong C.S., Li D.X. et al.: Development of Polyvinyl Alcohol–Sodium Alginate Gel-Matrix--Based Wound Dressing System Containing Nitrofurazone. International Journal of Pharmaceutics 359 (2008) 79-86, doi:10.1016/j.ijpharm.2008.03.021.
[12] Liang L., Hou T., Ouyang Q., Xie L., Zhong S., Li P., Li S., Li C.-P.: Antimicrobial Sodium Alginate Dressing Immobilized with Polydopamine-Silver Composite Nanospheres. Composites Part B: Engineering 188 (2020) 107877, doi:10.1016/j.compositesb.2020.107877.
[13] Pandima Devi M., Sekar M., Chamundeswari M., Moorthy A., Krithiga G., Murugan N.S., Sastry T.P.: A Novel Wound Dressing Material—Fibrin–Chitosan–Sodium Alginate Composite Sheet. Bulletin of Materials Science 35 (2012) 1157-1163, doi:10.1007/s12034-012-0404-5.
[14] Wu Z., Li Q., Xie S., Shan X., Cai Z.: In Vitro and in Vivo Biocompatibility Evaluation of a 3D Bioprinted Gelatin-Sodium Alginate/Rat Schwann-Cell Scaffold. Materials Science and Engineering: C 109 (2020) 110530, doi:10.1016/j.msec.2019.110530.
[15] Chung C.-W., Kang J.Y., Yoon I.-S., Hwang H.-D., Balakrishnan P., Cho H.-J. et al.: Interpenetrating Polymer Network (IPN) Scaffolds of Sodium Hyaluronate and Sodium Alginate for Chondrocyte Culture. Colloids and Surfaces B: Biointerfaces 88 (2011) 711-716, doi:10.1016/j.colsurfb.2011.08.005.
[16] Wang Y., Wang X., Shi J., Zhu R., Zhang J., Zhang Z. et al.: A Biomimetic Silk Fibroin/Sodium Alginate Composite Scaffold for Soft Tissue Engineering. Scientific Reports 6 (2016) 39477, doi:10.1038/srep39477.
[17] Xia H., Zhao D., Zhu H., Hua Y., Xiao K., Xu Y. et al.: Lyophilized Scaffolds Fabricated from 3D-Printed Photocurable Natural Hydrogel for Cartilage Regeneration. ACS Applied Materials & Interfaces 10 (2018) 31704-31715, doi:10.1021/acsami.8b10926.
[18] Odziomek K., Drabczyk A.K., Kościelniak P., Konieczny P., Barczewski M., Bialik-Wąs K.: The Role of Freeze-Drying as a Multifunctional Process in Improving the Properties of Hydrogels for Medical Use. Pharmaceuticals 17 (2024) 1512, doi:10.3390/ph17111512.
[19] Guziewicz N., Best A., Perez-Ramirez B., Kaplan D.L.: Lyophilized Silk Fibroin Hydrogels for the Sustained Local Delivery of Therapeutic Monoclonal Antibodies. Biomaterials 32 (2011) 2642-2650, doi:10.1016/j.biomaterials.2010.12.023.
[20] Fereshteh Z.: Freeze-Drying Technologies for 3D Scaffold Engineering. In: Deng Y., Kuiper J. (Eds.) Functional 3D Tissue Engineering Scaffolds, wyd. Woodhead Publishing, Cambridge 2018.
[21] Autissier A., Visage C.L., Pouzet C., Chaubet F., Letourneur D.: Fabrication of Porous Polysaccharide-Based Scaffolds Using a Combined Freeze-Drying/Cross-Linking Process. Acta Biomaterialia 6 (2010) 3640-3648, doi:10.1016/j.actbio.2010.03.004.
[22] Abla K.K., Mehanna M.M.: Freeze-Drying: A Flourishing Strategy to Fabricate Stable Pharmaceutical and Biological Products. International Journal of Pharmaceutics 628 (2022) 122233, doi:10.1016/j.ijpharm.2022.122233.
[23] Yavuz M., Erginer M., Kasavi C., Toksoy Oner E.: Enhanced Preservation of Viability and Species Stratification in Lacticaseibacillus Group Using Levan-Fortified Skim Milk as a Cryoprotectant during Freeze-Drying. Food Science and Biotechnology 34 (2025) 1605-1616, doi:10.1007/s10068-024-01802-x.
[24] Sun Y., Xie Y., Zou H., Chen Y., Wen Z., Liang Q. et al.: Fabrication and Application of Multifunctional Conductive Hydrogel Film for Wearable Sensors via Efficient Freeze-Thaw Cycling and Annealing Process. Chemical Engineering Journal 495 (2024) 153487, doi:10.1016/j.cej.2024.153487.
[25] Muhoza B., Yuyang H., Uriho A., Harindintwali J.D., Liu Q., Li Y.: Spray- and Freeze-Drying of Microcapsules Prepared by Complex Coacervation Method: A Review. Food Hydrocolloids 140 (2023) 108650, doi:10.1016/j.foodhyd.2023.108650.
[26] Bialik-Wąs K., Miastkowska M., Sapuła P., Pluta K., Malina D., Chwastowski J., Barczewski M.: Bio-Hybrid Hydrogels Incorporated into a System of Salicylic Acid-pH/Thermosensitive Nanocarriers Intended for Cutaneous Wound-Healing Processes. Pharmaceutics 14 (2022) 773, doi:10.3390/pharmaceutics14040773.
[27] Palmese L.L., Thapa R.K., Sullivan M.O., Kiick K.L.: Hybrid Hydrogels for Biomedical Applications. Current Opinion in Chemical Engineering 24 (2019) 143-157, doi:10.1016/j.coche.2019.02.010.

[28] Chircov C., Ioniță D.-A., Sîrmon A.-M., Neacșu I.A., Ficai A.: Natural, Synthetic, Hybrid and Composite Biomaterials for Neural Tissue Engineering. In: Gunduz O., Ustundag C.B., Sengor M. (Eds.) Biomaterials for Neural Tissue Engineering, wyd. Woodhead Publishing, Cambridge 2023.
[29] Luo M., Shaitan K., Qu X., Bonartsev A.P., Lei B.: Bioactive Rare Earth-Based Inorganic-Organic Hybrid Biomaterials for Wound Healing and Repair. Applied Materials Today 26 (2022) 101304, doi:10.1016/j.apmt.2021.101304.
[30] Jiang Y.-Y., Zhu Y.-J., Li H., Zhang Y.-G., Shen Y.-Q., Sun T.-W., Chen F.: Preparation and Enhanced Mechanical Properties of Hybrid Hydrogels Comprising Ultralong Hydroxyapatite Nanowires and Sodium Alginate. Journal of Colloid and Interface Science 497 (2017) 266-275, doi:10.1016/j.jcis.2017.03.032.
[31] Chang S., Wang J., Xu N., Wang S., Cai H., Liu Z., Wang X.: Facile Construction of Hybrid Hydrogels with High Strength and Biocompatibility for Cranial Bone Regeneration. Gels 8 (2022) 745, doi:10.3390/gels8110745.
[32] Hu C., Wang M.X., Sun L., Yang J.H., Zrínyi M., Chen Y.M.: Dual-Physical Cross-Linked Tough and Photoluminescent Hydrogels with Good Biocompatibility and Antibacterial Activity. Macromolecular Rapid Communications 38 (2017) 1600788, doi:10.1002/marc.201600788.
[33] Wang L., Zhou M., Xu T., Zhang X.: Multifunctional Hydrogel as Wound Dressing for Intelligent Wound Monitoring. Chemical Engineering Journal 433 (2022) 134625, doi:10.1016/j.cej.2022.134625.
[34] Teoh J.H., Mozhi A., Sunil V., Tay S.M., Fuh J., Wang C.-H.: 3D Printing Personalized, Photocrosslinkable Hydrogel Wound Dressings for the Treatment of Thermal Burns. Advanced Functional Materials 31 (2021) 2105932, doi:10.1002/adfm.202105932.
[35] Tan X., Feldman S.R., Chang J., Balkrishnan R.: Topical Drug Delivery Systems in Dermatology: A Review of Patient Adherence Issues. Expert Opinion on Drug Delivery 9 (2012) 1263-1271, doi:10.1517/17425247.2012.711756.
[36] Catoira M.C., Fusaro L., Di Francesco D., Ramella M., Boccafoschi F.: Overview of Natural Hydrogels for Regenerative Medicine Applications. Journal of Materials Science: Materials in Medicine 30 (2019) 115, doi:10.1007/s10856-019-6318-7.
[37] Lee K.Y., Mooney D.J.: Hydrogels for Tissue Engineering. Chemical Reviews 101 (2001) 1869-1880, doi:10.1021/cr000108x.
[38] Polley H.F., Mason H.L.: Rheumatoid Arthritis: Effects of Certain Steroids Other Than Cortisone and of Some Adrenal Cortex Extracts. Journal of the American Medical Association 143 (1950) 1474-1481, doi:10.1001/jama.1950.02910520016007.
[39] Sulzberger M.B., Witten V.H.: The Effect of Topically Applied Compound F in Selected Dermatoses. Journal of Investigative Dermatology 19 (1952) 101-102, doi:10.1038/jid.1952.72.
[40] Witten V.H., Amler A.B., Sulzberger M.B., DeSanctis A.G.: Hydrocortisone Ointment in the Treatment of Infantile Eczema. American Journal of Diseases of Children 87 (1954) 298-304, doi:10.1001/archpedi.1954.02050090286004.
[41] Sulzberger M.B., Witten V.H.: Hydrocortisone Ointment in Dermatological Therapy. Medical Clinics of North America 38 (1954) 321-336, doi:10.1016/S0025-7125(16)34877-5.
[42] Sulzberger M.B., Witten V.H.: Prolonged Therapy with Cortisone for Chronic Skin Diseases. Journal of the American Medical Association 155 (1954) 954-959, doi:10.1001/jama.1954.03690290004002.
[43] Friedlaender S., Friedlaender A.S.: Oral Cortisone Therapy in Allergic Disease. Journal of Allergy 22 (1951) 291-303, doi:10.1016/0021-8707(51)90030-5.
[44] Feinberg S.M., Dannenberg T.B., Malkiel S.: ACTH and Cortisone in Allergic Manifestations; Therapeutic Results and Studies on Immunological and Tissue Reactivity. Journal of Allergy 22 (1951) 195-210, doi:10.1016/0021-8707(51)90015-9.
[45] Bangham A.D.: The Effect of Cortisone on Wound Healing. British Journal of Experimental Pathology 32 (1951) 77-84.
[46] Jaeger M., Harats M., Kornhaber R., Aviv U., Zerach A., Haik J.: Treatment of Hypergranulation Tissue in Burn Wounds with Topical Steroid Dressings: A Case Series. International Medical Case Reports Journal 9 (2016) 241-245, doi:10.2147/IMCRJ.S113182.
[47] Hughes J., Rustin M.: Corticosteroids. Clinics in Dermatology 15 (1997) 715-721, doi:10.1016/S0738-081X(97)00020-5.
[48] Oakley R.H., Cidlowski J.A.: Homologous Down-Regulation of the Glucocorticoid Receptor: The Molecular Machinery. Critical Reviews in Eukaryotic Gene Expression 3 (1993) 63-88.
[49] Nicolaides N.C., Charmandari E., Chrousos G.P., Kino T.: Recent Advances in the Molecular Mechanisms Determining Tissue Sensitivity to Glucocorticoids: Novel Mutations, Circadian Rhythm and Ligand-Induced Repression of the Human Glucocorticoid Receptor. BMC Endocrine Disorders 14 (2014) 71, doi:10.1186/1472-6823-14-71.
[50] Cain D.W., Cidlowski J.A.: Immune Regulation by Glucocorticoids. Nat. Rev. Immunol. 17 (2017) 233-247, doi:10.1038/nri.2017.1.
[51] Ignarro L.J.: Glucocorticosteroid Inhibition of Nonphagocytic Discharge of Lysosomal Enzymes from Human Neutrophils. Arthritis & Rheumatism 20 (1977) 73-83, doi:10.1002/art.1780200114.
[52] Hengge U.R., Ruzicka T., Schwartz R.A., Cork M.J.: Adverse Effects of Topical Glucocorticosteroids. Journal of the American Academy of Dermatology 54 (2006) 1-15, doi:10.1016/j.jaad.2005.01.010.
[53] Cevc G., Blume G.: Hydrocortisone and Dexamethasone in Very Deformable Drug Carriers Have Increased Biological Potency, Prolonged Effect, and Reduced Therapeutic Dosage. Biochimica et Biophysica Acta – Biomembranes 1663 (2004) 61-73, doi:10.1016/j.bbamem.2004.01.006.
[54] Chen S., Jiang X., Sun L.: Reaction Mechanisms of N-Isopropylacrylamide Soap-Free Emulsion Polymerization Based on Two Different Initiators. Journal of Macromolecular Science – Part A 51 (2014) 447-455, doi:10.1080/10601325.2014.893144.
[55] Yan X., Gemeinhart R.A.: Cisplatin Delivery from Poly(Acrylic Acid-co-Methyl Methacrylate) Microparticles. Journal of Controlled Release 106 (2005) 198-208, doi:10.1016/j.jconrel.2005.05.005.
[56] Bialik-Wąs K., Miastkowska M., Sapuła P., Sycz A., Pluta K., Malina D., Chwastowski J.: Kinetic Analysis of in Vitro Release Profiles of Salicylic Acid and Fluocinolone Acetonide from Dual Delivery Systems Composed of Polymeric Nanocarriers and a Hydrogel Matrix. Journal of Drug Delivery Science and Technology 92 (2024) 105355, doi:10.1016/j.jddst.2024.105355.
[57] Bialik-Wąs K., Malina D., Pluta K., Miastkowska M.: Sposób Wprowadzania Hydrofobowych Leczniczych Substancji Czynnych, Tworzących Układ z Termoczułym Nanonośnikiem, do Hydrofilowej Matrycy Opatrunku Hydrożelowego. Patent PL 2021.
[58] Bialik-Wąs K., Pluta K., Malina D., Barczewski M., Malarz K., Mrozek-Wilczkiewicz A.: Advanced SA/PVA-Based Hydrogel Matrices with Prolonged Release of Aloe Vera as Promising Wound Dressings. Materials Science and Engineering: C 120 (2021) 111667, doi:10.1016/j.msec.2020.111667.
[59] Bialik-Wąs K., Królicka E., Malina D.: Impact of the Type of Crosslinking Agents on the Properties of Modified Sodium Alginate/Poly(vinyl Alcohol) Hydrogels. Molecules 26 (2021) 2381, doi:10.3390/molecules26082381.
[60] Bialik-Wąs K., Pluta K., Malina D., Barczewski M., Malarz K., Mrozek-Wilczkiewicz A.: The Effect of Glycerin Content in Sodium Alginate/Poly(vinyl Alcohol)-Based Hydrogels for Wound Dressing Application. International Journal of Molecular Sciences 22 (2021) 12022, doi:10.3390/ijms222112022.
[61] Bialik-Wąs K., Raftopoulos K.N., Pielichowski K.: Alginate Hydrogels with Aloe Vera: The Effects of Reaction Temperature on Morphology and Thermal Properties. Materials 15 (2022) 748, doi:10.3390/ma15030748.
[62] Bialik-Wąs K., Malina D., Pluta K.: Sposób Otrzymywania Hydrożelowych Materiałów Opatrunkowych. Patent PL 2020.
[63] Ahmed E.M.: Hydrogel: Preparation, Characterization, and Applications – A Review. Journal of Advanced Research 6 (2015) 105-121, doi:10.1016/j.jare.2013.07.006.
[64] Peppas N.A., Khare A.R.: Preparation, Structure and Diffusional Behavior of Hydrogels in Controlled Release. Advanced Drug Delivery Reviews 11 (1993) 1-35, doi:10.1016/0169-409X(93)90025-Y.
[65] Khan S., Ranjha N.M.: Effect of Degree of Cross-Linking on Swelling and on Drug Release of Low Viscous Chitosan/Poly(vinyl Alcohol) Hydrogels. Polymer Bulletin 71 (2014) 2133-2158, doi:10.1007/s00289-014-1178-2.
[66] Lee K.Y., Rowley J.A., Eiselt P., Moy E.M., Bouhadir K.H., Mooney D.J.: Controlling Mechanical and Swelling Properties of Alginate Hydrogels Independently by Cross-Linker Type and Cross-Linking Density. Macromolecules 33 (2000) 4291-4294, doi:10.1021/ma9921347.
[67] Pal K., Banthia A.K., Majumdar D.K.: Polymeric Hydrogels: Characterization and Biomedical Applications. Designed Monomers and Polymers 12 (2009) 197-220, doi:10.1163/156855509X436030.
[68] Biological Evaluation of Medical Devices - Part 5: Tests for in Vitro Cytotoxicity: In ANSI/AAMI/ISO 10993-5:2009/(R)2014, wyd. Arlington, USA 2009.